Chinese Herbal Medicines 17 (2025) 139–147

Contents lists available at ScienceDirect

Chinese Herbal Medicines

journal homepage: www.elsevier.com/locate/chmed

Original Article

Qishen Granule protects against myocardial ischemia by promoting angiogenesis through BMP2-Dll4-Notch1 pathway

Yiqin Hong [a,1], Hui Wang [a,1], Hanyan Xie [a,1], Xinyi Zhong [a], Xu Chen [b], Lishuang Yu [b], Yawen Zhang [b], Jingmei Zhang [a], Qiyan Wang [a], Binghua Tang [a], Linghui Lu [b,*], Dongqing Guo [a,*]

[a] School of Life Sciences, Beijing University of Chinese Medicine, Beijing 100029, China
[b] School of Traditional Chinese Medicine, Beijing University of Chinese Medicine, Beijing 100029, China

ARTICLE INFO

Article history:
Received 22 July 2023
Revised 12 October 2023
Accepted 23 December 2023
Available online 30 April 2024

Keywords:
angiogenesis
bone morphogenetic protein-2
delta-like 4
myocardial ischemia
notch homolog 1
Qishen Granule

ABSTRACT

Objective: Therapeutic angiogenesis has become a promising approach for treating ischemic heart disease (IHD). The present study aims to investigate the effects of Qishen Granule (QSG) on angiogenesis in myocardial ischemia (MI) and the potential mechanism.

Methods: *In vivo* study was conducted on rat model of myocardial infarction. QSG was performed daily at a dose of 2.352 g/kg for four weeks. Cardiac function was assessed by echocardiogram and pro-angiogenic effects were evaluated by Laser Doppler and CD31 expression. Oxygen-glucose deprivation (OGD) was applied in cultured human umbilical vein endothelial cells (HUVECs). Cell viability, wound healing and tube formation assay were used to test functions of HUVECs. ELISA and Western blots were used to assess protein expressions of bone morphogenetic protein 2-delta-like 4-notch homolog 1 (BMP2-Dll4-Notch1) signaling pathway.

Results: The results showed that QSG improved heart function, cardiac blood flow and microvessel density in myocardial ischemic rats. *In vitro,* QSG protected HUVECs by promoting the cell viability and tube formation. QSG upregulated bone morphogenetic protein-2 (BMP2) and downregulated delta-like 4 (Dll4) and notch homolog 1 (Notch1) expressions both in rats and HUVECs.

Conclusion: QSG protected against MI by promoting angiogenesis through BMP2-Dll4-Notch1 pathway. BMP2 might be a promising therapeutic target for IHD.

1. Introduction

Ischemic heart disease (IHD) contributes to be one of the most common reasons for morbidity and mortality worldwide (Aljefree, Lee, Alsaqqaf, & Ahmed, 2016). It brings not only endless suffering to patients, but also heavy burden to society and economy (Katz & Gavin, 2019). Thus it remains to be a scientific mission to develop effective treatments for IHD.

The current treatment of IHD mainly includes drug therapy, interventional therapy and coronary artery bypass grafting (Antman & Braunwald, 2020; Sabatine et al., 2005). Anti-platelet drugs, β-receptor blockers and statins are often used to stabilize the disease and reduce the incidence of acute events (Antman & Braunwald, 2020). Interventional therapy and coronary artery bypass grafting are two common surgical methods for vascular reconstruction. However, for patients with subepicardial and terminal vascular diffuse lesions, revascularization may not be achieved by these two methods (Caliskan, Falk, & Emmert, 2019; Fihn et al., 2014; Mitsos et al., 2012; Neumann et al., 2019). Therapeutic angiogenesis, a novel research hotspot, has played vital roles in IHD treatment. It has been proved to promote the establishment of collateral circulation and increase blood supply through the transmission of cytokines, genes, stem/progenitor cells, exosomes and so on in ischemic myocardium (Guo et al., 2018; Johnson, Zhao, Manuel, Taylor, & Liu, 2019; Sasaki et al., 2002). Recently, traditional Chinese medicine (TCM) has attracted more and more attention in the field of therapeutic angiogenesis for IHD. A lot of monomers, Chinese herbal formulas and Chinese patent drugs have been reported to be effective in the treatment of IHD through promoting angiogenesis (Guo et al., 2018). For example, Tanshinone IIA, an extract of *Salviae Miltiorrhizae Radix* et *Rhizoma* (Danshen in Chinese), could promote angiogenesis after myocardial ischemia (MI) by regulating miR-499-5p/PTEN pathway (Wang & Wu, 2022). Buyang Huanwu Decoction promoted

* Corresponding authors.
E-mail addresses: lulinghui@bucm.edu.cn (L. Lu), dong_qing_guo@126.com (D. Guo).
[1] These authors contributed equally to this work.

https://doi.org/10.1016/j.chmed.2023.12.007
1674-6384/

angiogenesis by activating PI3K/AKT/GSK3β pathway (Han et al., 2022). Shexiang Tongxin Dropping Pills accelerated angiogenesis by upregulating PI3K/AKT/mTORC1 pathway (Lu et al., 2022).

Bone morphogenetic proteins (BMPs) belong to transforming growth factors-β (TGF-β) family members and play an important role in intravascular homeostasis and angiogenesis independent of vascular endothelial growth factor (VEGF) (Lowery & Rosen, 2018). BMP2 has been reported to activate endothelial cells and promote angiogenesis (Zuo et al., 2016). Delta-like 4-notch homolog 1 (Dll4-Notch1) pathway is a highly conserved signal pathway that widely exists on the cell surface and is regulated by the receptor ligand mode (Pitulescu et al., 2017). Dll4 is a ligand of Notch mainly expressed on vascular endothelium, which mediates Notch1 signal pathway to participate in regulating angiogenesis (Pulkkinen et al., 2021).

Qishen Granule (QSG) is reformed from Zhenwu Decoction and Simiao Yong'an Decoction (Zeng et al., 2019; Liu et al., 2022). The formula of QSG is composed of *Astragali Radix* (Huangqi in Chinese), *Salviae Miltiorrhizae Radix* et *Rhizoma*, *Aconm Lateralis Radix Praeparaia* (Fuzi in Chinese), *Scrophulariae Radix* (Xuanshen in Chinese), *Lonicerae Japonicae Flos* (Jinyinhua in Chinese) and *Glycyrrhizae Radix* et *Rhizoma* (Gancao in Chinese) (Zeng et al., 2019). The composition is simple and the effect is definite (Liu et al., 2019). Our previous results showed that QSG could regulate metabolism (Yang et al., 2020), inhibit inflammatory activation (Chen et al., 2022) and myocardial fibrosis (Zeng et al., 2019). However, the protective effects and mechanism of QSG on angiogenesis are still unknown. In this paper, we investigated the effects of QSG on angiogenesis in IHD and tested the potential mechanism via BMP2-Dll4-Notch1 pathway.

2. Materials and methods

2.1. Herbs preparation

QSG were composed of 460 g *Astragali Radix*, 230 g *Salviae Miltiorrhizae Radix* et *Rhizoma*, 160 g *Lonicerae Japonicae Flos*, 160 g *Scrophulariae Radix*, 140 g *Aconm Lateralis Radix Praeparaia*, and 90 g *Glycyrrhizae Radix* et *Rhizoma*. These herbs were purchased from Beijing Tongrentang Chinese Medicine Co., Ltd. (Beijing, China) and prepared as reported previously. The fingerprint spectrum was further established by the high performance liquid chromatography (HPLC) in our previous studies (Xia et al., 2017).

2.2. Animals

All experimental procedures were carried out according to the procedures approved by the Animal Protection and Utilization Committee of Beijing University of Chinese Medicine (approval number: BUCM-4-2018001201-1014). Sprague-Dawley (SD) rats (250 g) were provided by SPF Biotechnology Co., Ltd. (SCXK2019-0010, Beijing, China). The left anterior descending artery of SD rats was ligated to induce MI model as described previously (Chen et al., 2021). The survived rats were divided randomly into model group, QSG group (2.352 g/kg) and rosuvastatin group (1 mg/kg), with 10 rats in each group. The dose of QSG was chosen according to our previous study (Zhang et al., 2020). The dose of rosuvastatin was referring to clinical application and calculated by the equivalent conversion between human and rats. The control group was set as a control. All rats received drug or vehicle daily via oral gavage since day 1 post-MI/sham surgery till 4th weeks. All animal experiments were carried out in accordance with the UK Animals (Scientific Procedures) Act, 1986 and EU Directive 2010/63/EU guidelines and regulations (Kilkenny, Browne, Cuthill, Emerson, & Altman, 2010).

2.3. Echocardiography

Echocardiography (Vevo TM 2100, Visual Sonics, Toronto, Canada) was applied to evaluate the cardiac functions. Echocardiography detection was performed from parasternal short axis at papillary muscle level in anesthetized rats. The parameters measured and calculated from echo-vedios were as follows: left ventricular end-diastolic diameter (LVID; d), left ventricular end-systolic diameter (LVID; s), fractional shortening (FS) and ejection fraction (EF).

2.4. Cardiac micro blood flow (MBF) scan

After 12 h of fasting, all rats were anesthetized. The left chest was opened and the heart was exposed, the scanning probe was placed parallel to the surface of the heart at a distance of 5 cm. The light beam at each measurement point irradiated the tissue to a depth of 0.5 mm. Cardiac blood flow was measured using moorFLPI-2 blood flow imager (Moor Instruments, Axminster, UK). The images with blue to red indicated low to high blood flow.

2.5. Haematoxylin-eosin (HE) staining

Fresh heart samples were fixed in 4% paraformaldehyde, embedded in paraffin and cut into slices to 5 μm. The slices were stained with HE. The results were observed under an optical microscope.

2.6. Immunofluorescence determination

The tissue sections were dewaxed, repaired with sodium citrate antigen retrieval solution, blocked by 5% bovine serum albumin (BSA) for 1 h, incubated with anti-CD31 antibody (28083–1-AP, ProteinTech) overnight at 4 °C, secondary antibody incubated for 1 h, nuclei stained with 4′,6-diamidino-2-phenylindole (DAPI), and observed under confocal microscopy.

2.7. Cell culture and cell viability assay

Human umbilical vein endothelial cells (HUVECs) were obtained from Beijing Anzhen Hospital and cultured with a 1640 medium containing 10% fetal bovine serum (FBS) and 1% penicillin/streptomycin (P/S) in a humidified incubator with 5% CO_2 at 37 °C. HUVECs were divided into the control group, model group and QSG groups. When HUVECs were cultured to 80%−90% confluence, oxygen-glucose deprivation (OGD) model was performed as described below. Cells in the model group were washed with PBS twice and then incubated in Earle's balanced salt solution to imitate glucose deprivation. After washing, the QSG groups were incubated in Earle's balanced salt solution mixed with different concentrations of QSG (10−2 000 μg/mL). Then the plate was placed in an anoxic incubator for 8 h. After different treatments, the original medium was discarded and CCK-8 solution was added to each well and incubated for 2 h at 37 °C in the dark. The absorbance was measured by PerkinElmer microplate reader (PerkinElmer VICTOR 1420, Waltham, USA) at 450 nm.

2.8. siRNA transfection

BMP2 expression was knocked down using BMP2 si-RNA (GenePharma, Shanghai, China) according to the manufacturer's instructions. Briefly, HUVECs were incubated with 500 μL RNAfit and 10 μL si-RNA for 6 h, and then, the medium was replaced by 1640 (5% FBS; P/S free) for another 34 h. Cells transfected with non-specific si-RNA were used as control group (NC group). The sequence of siRNA-1 (5′−3′) was GCUGUACCUUGACGAGAAUTT; AUUCUCGUCAAGGUACAGCTT. The sequence of siRNA-2 (5′−3′)

was GCAGUUUCCAUCACCGAAUTT; AUUCGGUGAUGGAAACUGCTT. The sequence of siRNA-3 (5′–3′) was CCCGGAGAUUCUUCUUUAATT; UUAAAGAAGAAUCUCCGGGTT. The sequence of NC siRNA (5′–3′) was UUCUCCGAACGUGUCACGUTT; ACGUGACACGUUCGGAGAATT.

2.9. Wound healing assay

When HUVECs were cultured to 80%–90% confluence in a six-well plate, a line was gently drawn on the bottom of each well with a pipette tip and washed three times with PBS. The width of the scratch was observed under an inverted microscope (BX50-FLA, Olympus, Tokyo, Japan). The degree of the scratch healing by different treatments were calculated by the scratch area of 0 h and 8 h.

2.10. Tube formation assay

The 96-well plates were coated with 35 μL of growth factor reduced Matrigel (354230, Biocoat, Corning, USA). After different treatments, HUVECs were seeded at 1×10^6 cells/mL onto the Matrigel. After 5 h, the supernatant was discarded, and the cells

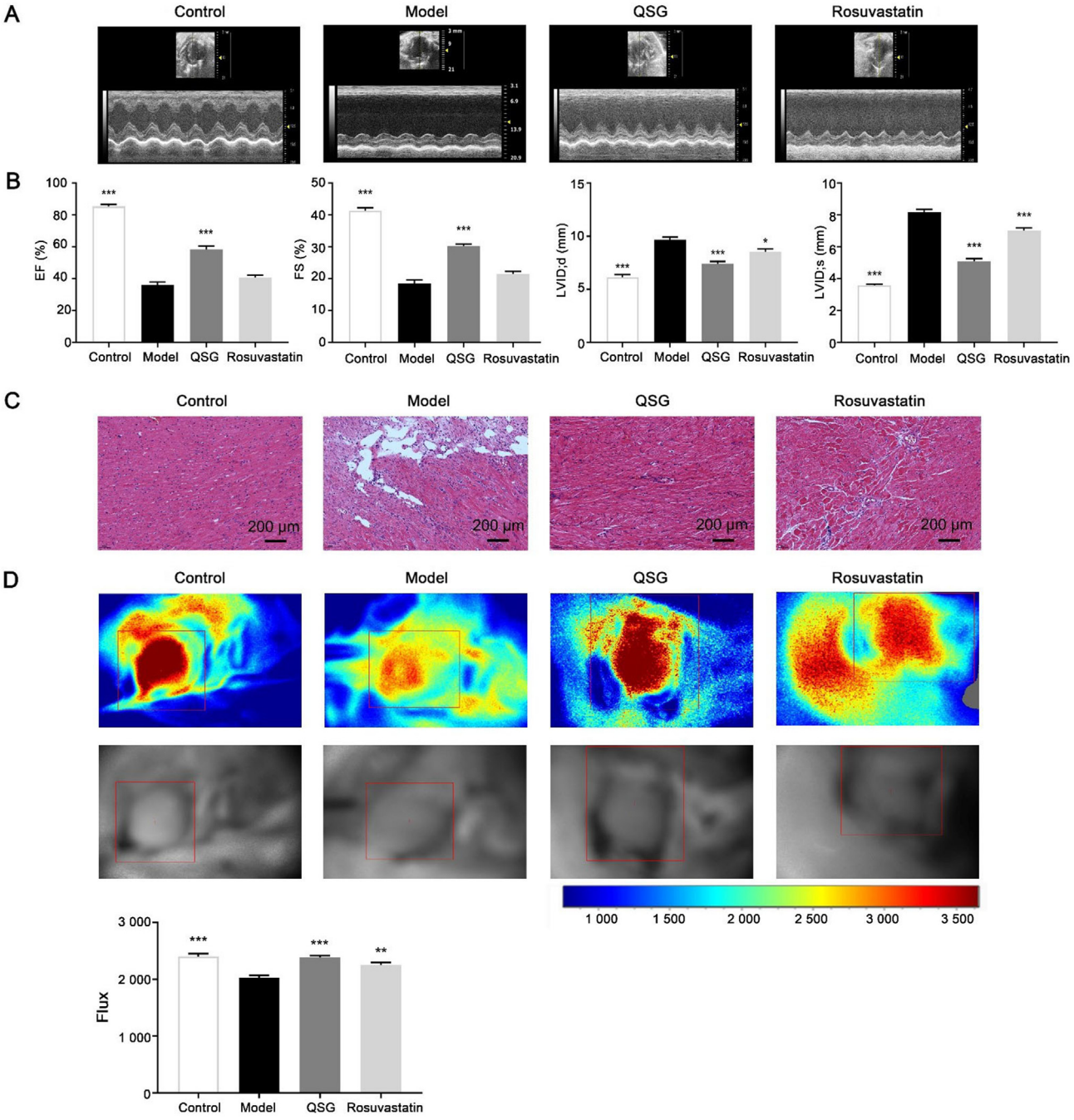

Fig. 1. QSG improved heart function and promoted cardiac angiogenesis. (A) Representative M-mode echocardiographic images in each group. (B) Quantitative analysis of EF, FS, LVID;d and LVID;s. (C) HE staining of heart tissue in different groups. (D) Representative cardiac micro blood flow of rat hearts from control group, model group, QSG group and rosuvastatin group. The more blood flow, the redder the color. Quantitative analysis of cardiac micro blood flow. Scale bar, 200 μm (× 100). Data were presented as mean ± SEM (n = 7). $^{*}P < 0.05$, $^{**}P < 0.01$, $^{***}P < 0.001$ *vs* model group.

were washed with PBS. Calcein-AM dye (5 μg/mL) was added and stained for 5 min. Photographs were taken using an inverted fluorescence microscope (SP8, Leica Microsystems CMS GmbH, Wetzlar, Germany). The total length of tubes and the total number of branch points in the picture were calculated by using Image-Pro Plus 6.0.

2.11. ELISA and western blot analysis

After different treatments, supernatant was collected to detect BMP2 by ELISA according to the manufacturer's instructions (Ruixin Biotech, Quanzhou, China).

Myocardial tissue and HUVECs were added with prepared RIPA lysate, fully lysed for 20 min, centrifuged at 12 000 r/min for 10 min, and supernatant was obtained. The loading buffer was added to adjust the protein concentration. After 10 min of metal bath at 98 °C, the protein was fully denatured and then used after natural cooling. Marker (5 μL) and protein sample (10 μL) were added into the sample hole of the prepared concentrated glue, which was separated at 110 V for 90 min, transferred at 300 mA for 90 min, and blocked with 5% milk for 2 h. The film was incubated in anti-BMP2 (YT5651; Immunoway), anti-Dll4 (bs-5909R; Bioss) and anti-Notch1 (10062–2-AP; ProteinTech) at 4 °C overnight, and anti-rabbit IgG H&L (ab16284; Abcam) was incubated at room temperature for 1 h. The film was placed in a gel imager, the luminescent liquid was uniformly dropped on the film, and the image was obtained and saved. Image Lab was used to calculate and analyze the strip ash.

2.12. Statistical analysis

Data are expressed as mean ± SEM of at least three independent experiments. One-way analysis of variance (ANOVA) was used for the statistical analysis of all the independent experiments. *P*-values less than 0.05 were considered statistical significance.

3. Results

3.1. QSG significantly improved cardiac function and cardiac blood flow

Four weeks after MI, echocardiography was conducted to assess cardiac function. As shown in (Fig. 1A and B), the heart cavity of the model group was enlarged, the apical area or the anterior heart wall became thinner, and the ventricular wall motion was weakened or disappeared, EF and FS values reduced by 57.73% and 55.06% compared with the control group. These alterations indicated that cardiac dysfunction and structural remodeling occurred in MI model group. After QSG administration, the levels of EF and FS were notably upregulated, while LVID;d and LVID;s were reduced significantly. HE staining showed that aberrant histological changes of cardiomyocyte were ameliorated in QSG treated rats (Fig. 1C). The positive drug rosuvastatin also showed protective effects on cardiac function. What's more, Laser Doppler was used to evaluate the pro-angiogenic effects of QSG. Laser Doppler results showed that red signal in QSG group was extremely stronger than that in the model group, indicating that cardiac micro blood flow (MBF) increased with sufficient blood supply after QSG treatment (Fig. 1D).

3.2. QSG regulated BMP2-Dll4-Notch1 pathway to promote angiogenesis in myocardial ischemic rats

We extracted protein from the border zone of infarcted heart of MI rats and tested the protein expressions of BMP2-Dll4-Notch1 pathway. Western blots results exhibited that BMP2 was diminished in the model group, while QSG could enhance the expression of BMP2 (Fig. 2A and B). Meanwhile the expressions of Dll4 and Notch1 were elevated in the model group compared to the control group. The administration of QSG attenuated the expressions of Dll4 and Notch1 compared to the model group. CD31, marker of vascular endothelium, were detected to evaluate vascular density

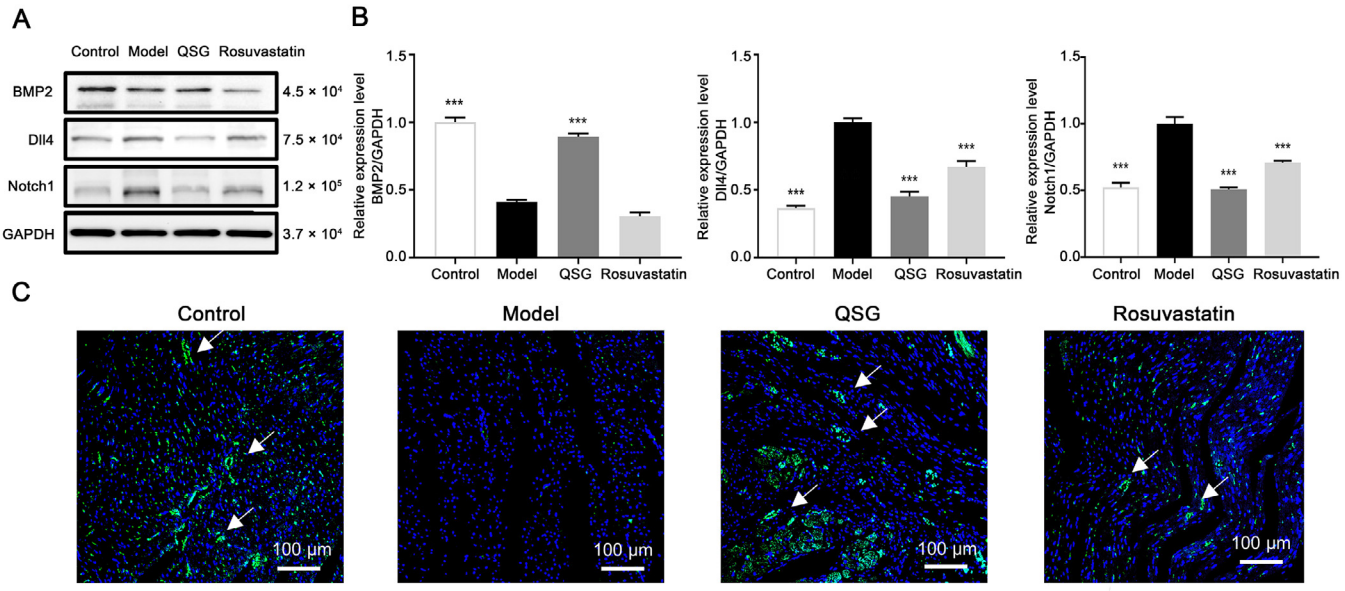

Fig. 2. Effects of QSG on angiogenesis of BMP2-Dll4-Notch1 pathway in myocardial ischemic rats. (A–B) Representative immunoblot images and quantitative analysis of BMP2, Dll4 and Notch1 in different groups. Glyceraldehyde-3-phosphate dehydrogenase (GAPDH) served as the internal control. (C) Representative immunofluorescent images were shown. CD31 was used to identify endothelial cells, DAPI to visualize cell nuclei. Scale bar, 100 μm (× 20). Data were presented as mean ± SEM (n = 3). $^{*}P < 0.05$, $^{**}P < 0.01$, $^{***}P < 0.001$ *vs* model group.

(Fig. 2C). The data showed that QSG regulated BMP2-Dll4-Notch1 pathway to promote angiogenesis in myocardial ischemic rats.

3.3. QSG protected endothelial cells from OGD induced injury

To investigate the effects of QSG on endothelial cells, HUVECs were treated with QSG at different concentrations *in vitro*. As measured by CCK-8 assay, QSG incubation had no toxic effect at a range of 10 μg/mL to 1000 μg/mL (Fig. 3A). OGD injury induced almost 40% reduction of cell viability which could be ameliorated significantly by QSG treatment at the concentration of 400 μg/mL to 800 μg/mL. The protective effects of QSG peaked at 600 μg/mL (Fig. 3B). The pro-angiogenesis effects of QSG were further examined using wound healing assay and tube formation assay. Compare with model group, QSG at 600 μg/mL not only could significantly reduce the scratch area, but also could increase the total length of the tube and the total number of branches. The results showed that QSG significantly stimulated the ability of HUVECs to migrate and form tube-like structures compared to model group (Fig. 3C and D).

3.4. QSG regulated protein expressions in BMP2-Dll4-Notch1 pathway in vitro

To further identify the potential mechanism of QSG in protecting OGD-induced endothelial cells, we examined the expressions of

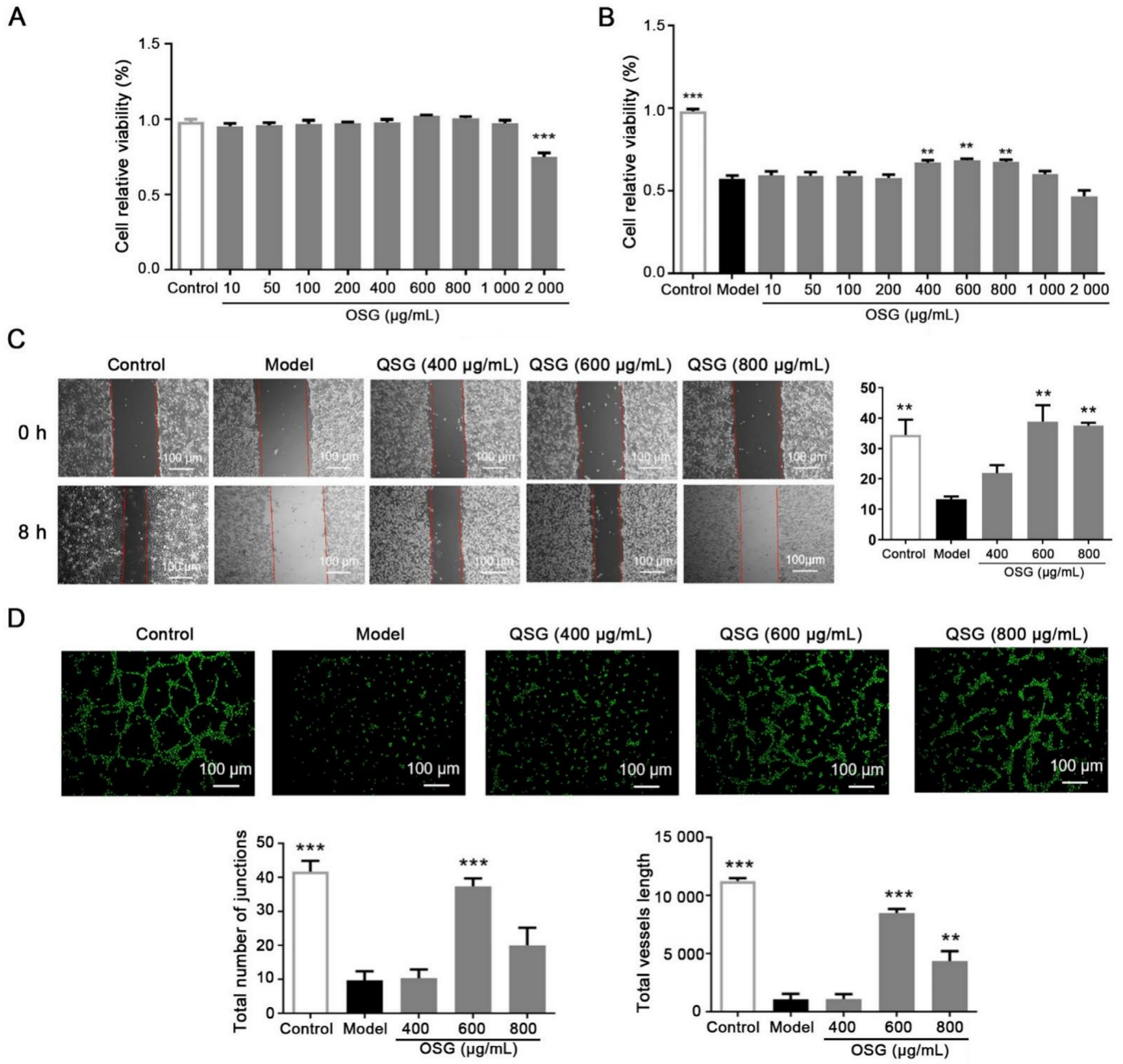

Fig. 3. QSG ameliorated survival rate and promoted angiogenesis in OGD-induced HUVECs model. (A–B) Safe concentration and efficacy of QSG on HUVECs were detected by CCK-8 assay. (C) QSG promoted cell migration in OGD-induced HUVECs. Cell migration capacity was assessed by ratio of scratch healing area to original area before and after the treatment. Scale bar, 100 μm (× 5). (D) Representative image of tube formation in different groups. Quantitative analysis of vessel branch points and vessel length were shown. Scale bar, 100 μm (× 10). Data were presented as mean ± SEM (n = 3). $^{*}P < 0.05$, $^{**}P < 0.01$, $^{***}P < 0.001$ *vs* model group.

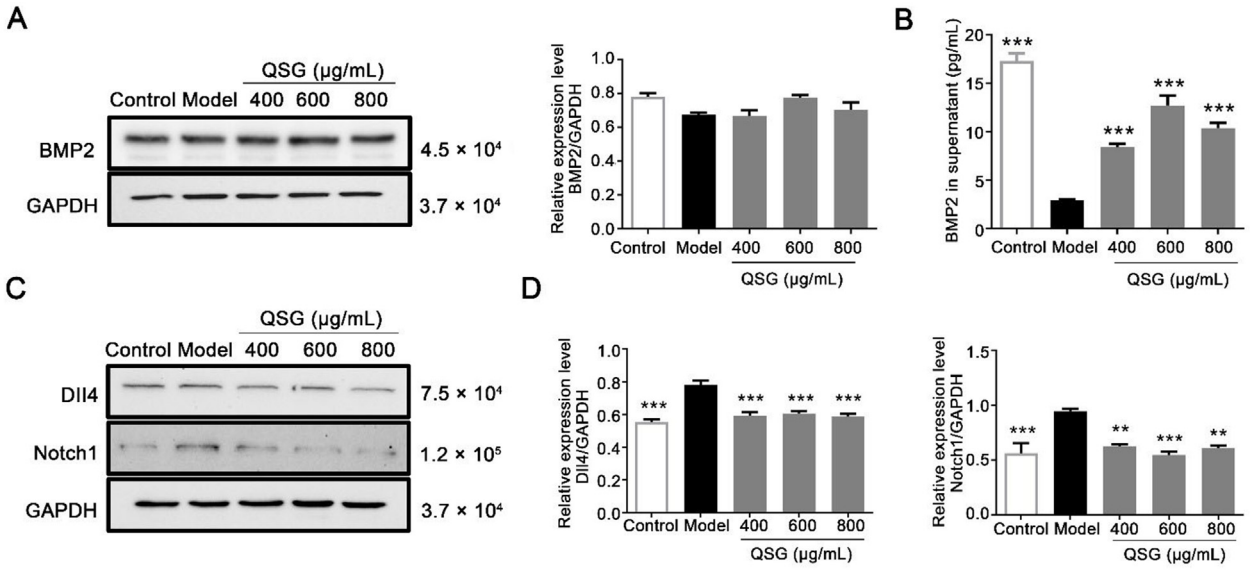

Fig. 4. Effects of QSG on protein expressions in BMP2-Dll4-Notch1 pathway in OGD-induced HUVECs model. (A) Expression of BMP2 in HUVECs detected by Western blots. (B) Release of BMP2 in supernatant of HUVECs detected by ELISA. (C–D) Representative immunoblots and corresponding quantification of Dll4 and Notch1 protein levels in HUVECs. Data were presented as mean ± SEM (n = 3). $^{**}P < 0.01$, $^{***}P < 0.001$ *vs* model group.

proteins related to angiogenesis. The expression of BMP2 protein did not change significantly in HUVECs detected by Western blots (Fig. 4A). Then the BMP2 levels in the supernatant of HUVECs were tested by ELISA. The results showed the secretion of BMP2 in the HUVEC supernatant decreased sharply in OGD cells while increased significantly in the presence of QSG at different concentrations (Fig. 4B). The downstream proteins of BMP2 were also detected by western blots. OGD obviously enhanced the expressions of Dll4 and Notch1 which were inhibited by treatment with 600 and 800 μg/mL QSG (Fig. 4C and D).

3.5. BMP2 knockdown attenuated pro-angiogenic ability of QSG in vitro

To investigate the key function of BMP2-Dll4-Notch1 pathway in pro-angiogenic effects of QSG, BMP2 was knocked down by siRNA in HUVECs. The knockdown efficiency of siRNA was verified by Western blots and siRNA-2 was chosen for the subsequent experiments (Fig. 5A). HUVECs were subjected by BMP2 knockdown prior to OGD stimulation. As shown in (Fig. 5B), si-RNA treatment markedly reduced BMP2 secretion in different groups compared to their own NC group. No statistical difference was further detected between QSG and model group after BMP2 si-RNA (Fig. 5B), indicating the pro-secretion effects of QSG was abolished by BMP-2 knockdown. In matrigel angiogenesis assay, QSG significantly stimulated the ability of HUVECs to form tube-like structures compared to the OGD group, and the pro-angiogenic ability of QSG disappeared after BMP2 si-RNA (Fig. 5C). To sum up, BMP2 si-RNA diminished the pro-angiogenetic effects of QSG on HUVECs.

4. Discussion

In this paper, our findings highlighted that QSG protected heart function against myocardial ischemic injury. *In vivo*, QSG increased cardiac blood flow and microvessel density significantly in ischemic rat heart. *In vitro*, QSG enhanced the cell viability, maintained the normal cell morphology, promoted the cell migration and tube formation in OGD-induced HUVECs. These results indicated that QSG protected against MI injury by promoting angiogenesis.

Therapeutic angiogenesis refers to the process of forming and developing new blood vessels on the basis of existing blood vessels (Li, Rochette, Wu, & Rosenblatt-Velin, 2019). The process of angiogenesis includes the activation, proliferation and migration of vascular endothelial cells, as well as the maturation and stability of newly formed buds (Todorova, Simoncini, Lacroix, Sabatier, & Dignat-George, 2017). In our experiment, we combined Laser Doppler and CD31 immunohistochemistry to evaluate the cardiac angiogenesis with the treatment of QSG. The overall blood flow of the heart surface was visualized and QSG could promote cardiac angiogenesis in MI rats compared to the model rats. Increased angiogenesis could promote the supply of nutrients and oxygen for impaired heart (Jabs et al., 2018). It has been reported that QSG exhibited evident cardio-protection via multiple pathways. Cardiac function can be preserved by QSG treatment through inhibiting calcium/calmodulin-dependent protein kinase II (CaMKII) and calcineurin (CaN) in the calcium signaling pathway (Yang et al., 2020). Fibrosis could be attenuated by QSG through inhibiting TGF-β1-Smad3 and PI3K-AKT-GSK-3β signaling pathways (Chen et al., 2022). In addition, QSG could regulate NF-κB-NLRP3-GSDMD signaling pathway to alleviate inflammasome activation and pyroptosis after MI (Chen et al., 2021). In this paper, we explored the effects of QSG on angiogenesis in MI rats and revealed the potential mechanism.

Emerging evidence indicated that BMPs were implicated in cardiac development (Dronkers, Wauters, Goumans, & Smits, 2020), vascular diseases (Cai, Pardali, Sánchez-Duffhues, & ten Dijke, 2012) and cancers (Sartori et al., 2021). BMP2 deletion in mice was linked to the cardiac development defects and embryonic lethality (Zhang & Bradley, 1996). The serum BMP2 decreased from 1 d after MI in patients, which coincided with the process of left ventricular remodeling (Sanders et al., 2016). What's more, BMP2 might participate in the angiogenesis (Dronkers, Wauters, Goumans, & Smits, 2020). BMP2 over-expression augmented the blood vessel formation in lung tumors of nude mice (Langenfeld and Langenfeld, 2004). BMP2 inhibitor was used to reverse the pro-angiogenic effects of BMP2 (Sanders et al., 2016). Knockdown the expression of BMP2 in hepatocarcinoma inhibited the

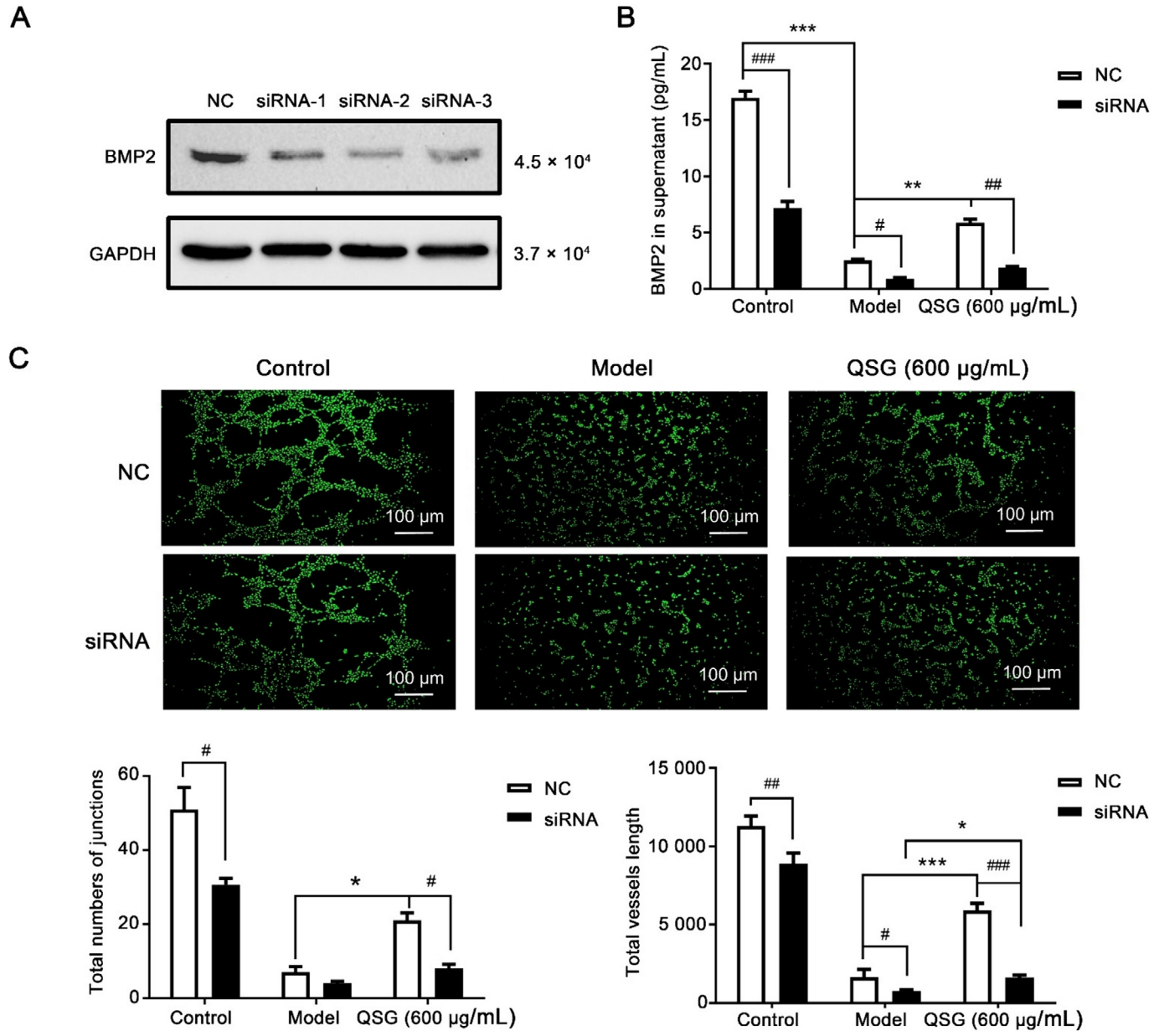

Fig. 5. Tube formation in OGD-induced HUVECs after BMP2 si-RNA treatment. (A) Immunoblotting to filter out most interference efficient si-RNA. (B) BMP2 levels in HUVEC supernatant detected by ELISA with/without BMP2 si-RNA treatment. (C) Tube formation reduced in OGD-induced HUVECs after BMP2 si-RNA. Quantitative analysis of vessel branch points and vessel length. Scale bar, 100 μm (× 10). Data were presented as mean ± SEM (n = 3). $^{*}P < 0.05$, $^{***}P < 0.001$ *vs* model group, $^{\#}P < 0.05$, $^{\#\#}P < 0.01$, $^{\#\#\#}P < 0.001$ *vs* NC group.

angiogenesis of HUVECs through P38, extracellular regulated protein kinases (ERK) and protein kinase B/mammalian target of rapamycin (AKT/mTOR) pathway (Zuo et al., 2016). Dll4 as a negative regulator of angiogenic sprouting (Lobov et al., 2007), could be induced by BMP2 (Benn et al., 2017). Notch1 is a highly conserved receptor that widely exists on the cell surface and is regulated by the receptor ligand mode by Dll4 (Pitulescu et al., 2017). Mats Hellstrom et al. found that inhibiting Dll4-Notch1 pathway could enhance tip cells formation during angiogenesis (Hellström et al., 2007). Activated Notch1 can release notch intracellular domain (NICD) into the nucleus and activate CBF1/suppressor of hairless/LaG1 (CSL) transcription factors, thereby inhibiting angiogenesis (Bridges et al., 2020).

In our study, we found that QSG regulated BMP2-Dll4-Notch1 pathway in myocardial ischemic rats and OGD-induced endothelial cells. *In vivo*, decreased BMP2 and increased Dll4 and Notch1 occurred in the model rats. QSG treatment could promote BMP2 expression, attenuate Dll4 and Notch1 expressions compared to the model group. Consistent results were verified *in vitro*. To further explore the effects of BMP2 on pro-angiogenic effects of QSG, si-RNA was used to knockdown the expression of BMP2 in HUVECs. The results showed that the facilitation of tube formation of QSG disappeared after BMP2 si-RNA, suggesting the pro-angiogenic effects of QSG might function by BMP2-Dll4-Notch1 pathway (Fig. 6). In this study, rosuvastatin was used as the positive drug. Rosuvastatin is a statin with hypolipidemic and anti-atherosclerotic effects, and can also be used clinically to prevent cardiovascular disease (Liao, Shen, & Liu, 2021). It has been reported that rosuvastatin could not only promote the formation of human umbilical vein endothelial cells *in vitro* experiments (Khaidakov et al., 2009), but also promote angiogenesis after acute myocardial infarction in rats (Sun, Wan, Song, & Sun, 2013). QSG as Chinese herbal compound has the characteristics of multi-components and multi-targets. The effect of rosuvastatin in

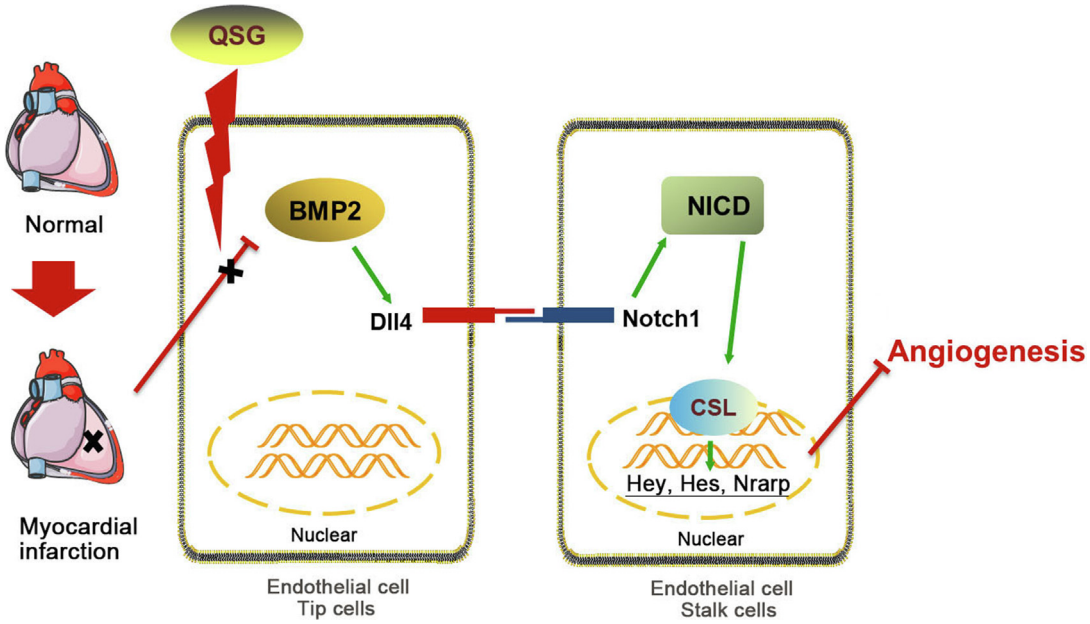

Fig. 6. Potential mechanism of QSG on angiogenesis against MI.

promoting angiogenesis was weaker than that of QSG in our experiments, which might be related to its single mechanism of action.

5. Conclusion

Collectively, our findings indicated that QSG protected against myocardial ischemic injury by promoting angiogenesis partly through BMP2-Dll4-Notch1 signaling pathway. Our study provides new targets for the treatment of IHD in clinic.

CRediT authorship contribution statement

Yiqin Hong: Investigation, Formal analysis, Writing – original draft. **Hui Wang:** Investigation, Formal analysis, Writing – original draft. **Hanyan Xie:** Investigation, Formal analysis, Writing – original draft. **Xinyi Zhong:** Investigation, Visualization. **Xu Chen:** Investigation. **Lishuang Yu:** Formal analysis. **Yawen Zhang:** Supervision. **Jingmei Zhang:** Supervision. **Qiyan Wang:** Writing – review & editing. **Binghua Tang:** Supervision. **Linghui Lu:** Writing – review & editing. **Dongqing Guo:** Supervision, Resources, Methodology, Funding acquisition, Writing – review & editing.

Declaration of competing interest

The authors declare that they have no known competing financial interests or personal relationships that could have appeared to influence the work reported in this paper.

Acknowledgments

This work was supported by the National Natural Science Foundation of China held by LL (No. 81904169) and Excellent Youth Foundation of BUCM held by DG (No. BUCM-2019-JCRC005).

References

Aljefree, N. M., Lee, P., Alsaqqaf, J. M., & Ahmed, F. (2016). Association between vitamin D status and coronary heart disease among adults in Saudi Arabia: A case-control study. *Healthcare (Basel, Switzerland), 4*(4), 77.

Antman, E. M., & Braunwald, E. (2020). Managing stable ischemic heart disease. *The New England Journal of Medicine, 382*(15), 1468–1470.

Benn, A., Hiepen, C., Osterland, M., Schütte, C., Zwijsen, A., & Knaus, P. (2017). Role of bone morphogenetic proteins in sprouting angiogenesis: Differential BMP receptor-dependent signaling pathways balance stalk vs. tip cell competence. *FASEB Journal: Official Publication of the Federation of American Societies for Experimental Biology, 31*(11), 4720–4733.

Bridges, E., Sheldon, H., Kleibeuker, E., Ramberger, E., Zois, C., Barnard, A., ... Harris, A. (2020). RHOQ is induced by DLL4 and regulates angiogenesis by determining the intracellular route of the Notch intracellular domain. *Angiogenesis, 23*(3), 493–513.

Cai, J., Pardali, E., Sánchez-Duffhues, G., & ten Dijke, P. (2012). BMP signaling in vascular diseases. *FEBS letters, 586*(14), 1993–2002.

Caliskan, E., Falk, V., & Emmert, M. Y. (2019). Multiarterial grafting in coronary artery bypass grafting. *European Heart Journal, 40*(30), 2479–2481.

Chen, X., Li, Y., Li, J., Liu, T., Jiang, Q., Hong, Y., ... Wang, Y. (2022). Qishen granule (QSG) exerts cardioprotective effects by inhibiting NLRP3 inflammasome and pyroptosis in myocardial infarction rats. *Journal of Ethnopharmacology, 285*, 114841.

Chen, X., Ma, L., Shao, M., Wang, Q., Jiang, Q., Guo, D., ... Wang, W. (2021). Exploring the protective effects of PNS on acute myocardial ischaemia-induced heart failure by transcriptome analysis. *Journal of Ethnopharmacology, 271*, 113823.

Dronkers, E., Wauters, M. M. M., Goumans, M. J., & Smits, A. M. (2020). Epicardial TGFβ and BMP signaling in cardiac regeneration: What lesson can we learn from the developing heart? *Biomolecules, 10*(3), 404.

Fihn, S. D., Blankenship, J. C., Alexander, K. P., Bittl, J. A., Byrne, J. G., Fletcher, B. J., ... Smith, P. K. (2014). 2014 ACC/AHA/AATS/PCNA/SCAI/STS focused update of the guideline for the diagnosis and management of patients with stable ischemic heart disease: A report of the American college of cardiology/American heart association task force on practice guidelines, and the American association for thoracic surgery, preventive cardiovascular nurses association, society for cardiovascular angiography and interventions, and society of thoracic surgeons. *Journal of the American College of Cardiology, 64*(18), 1929–1949.

Guo, D., Murdoch, C. E., Liu, T., Qu, J., Jiao, S., Wang, Y., ... Chen, X. (2018). Therapeutic angiogenesis of Chinese herbal medicines in ischemic heart disease: A review. *Frontiers in Pharmacology, 9*, 428.

Han, X., Zhang, G., Chen, G., Wu, Y., Xu, T., Xu, H., ... Zhou, Y. (2022). Buyang Huanwu Decoction promotes angiogenesis in myocardial infarction through suppression of PTEN and activation of the PI3K/Akt signalling pathway. *Journal of Ethnopharmacology, 287*, 114929.

Hellström, M., Phng, L. K., Hofmann, J. J., Wallgard, E., Coultas, L., Lindblom, P., ... Betsholtz, C. (2007). Dll4 signalling through Notch1 regulates formation of tip cells during angiogenesis. *Nature, 445*(7129), 776–780.

Jabs, M., Rose, A. J., Lehmann, L. H., Taylor, J., Moll, I., Sijmonsma, T. P., ... Fischer, A. (2018). Inhibition of endothelial Notch signaling impairs fatty acid transport and leads to metabolic and vascular remodeling of the adult heart. *Circulation, 137*(24), 2592–2608.

Johnson, T., Zhao, L., Manuel, G., Taylor, H., & Liu, D. (2019). Approaches to therapeutic angiogenesis for ischemic heart disease. *Journal of Molecular Medicine (Berlin, Germany), 97*(2), 141–151.

Katz, D., & Gavin, M. C. (2019). Stable ischemic heart disease. *Annals of Internal Medicine, 171*(3).

Khaidakov, M., Wang, W., Khan, J. A., Kang, B. Y., Hermonat, P. L., & Mehta, J. L. (2009). Statins and angiogenesis: Is it about connections? *Biochemical and Biophysical Research Communications, 387*(3), 543–547.

Kilkenny, C., Browne, W. J., Cuthill, I. C., Emerson, M., & Altman, D. G. (2010). Improving bioscience research reporting: The arrive guidelines for reporting animal research. *PLoS Biology, 8*(6), e1000412.

Langenfeld, E. M., & Langenfeld, J. (2004). Bone morphogenetic protein-2 stimulates angiogenesis in developing tumors. *Molecular Cancer Research, 2*(3), 141–149.

Li, N., Rochette, L., Wu, Y., & Rosenblatt-Velin, N. (2019). New insights into the role of exosomes in the heart after myocardial infarction. *Journal of Cardiovascular Translational Research, 12*(1), 18–27.

Liao, Y., Shen, X., & Liu, W. (2021). The effects of intensified lipid-lowering therapy with atorvastatin and rosuvastatin on blood lipid indicators, VEGF, and HCY levels in patients with acute cerebral infarction. *Clinical Medical Research and Practice, 6*(23), 55–57.

Liu, J., Li, Y., Zhang, Y., Huo, M., Sun, X., Xu, Z., ... Wang, W. (2019). A network pharmacology approach to explore the mechanisms of Qishen Granules in heart failure. *Medical Science Monitor: International Medical Journal of Experimental and Clinical Research, 25*, 7735–7745.

Liu, L. L., Li, Y. T., Su, R. B., Pan, Q. X., Wei, Z. Y., Qu, B. Q., ... Xiao, H. B. (2022). Chemical composition determination and consistency analysis of Qishen Granules based on liquid chromatography-mass spectrometry technology. *Chinese Traditional and Herbal Drugs, 53*(8), 2312–2323.

Lobov, I. B., Renard, R. A., Papadopoulos, N., Gale, N. W., Thurston, G., Yancopoulos, G. D., & Wiegand, S. J. (2007). Delta-like ligand 4 (Dll4) is induced by VEGF as a negative regulator of angiogenic sprouting. *Proceedings of the National Academy of Sciences of the United States of America, 104*(9), 3219–3224.

Lowery, J. W., & Rosen, V. (2018). The BMP pathway and its inhibitors in the skeleton. *Physiological Reviews, 98*(4), 2431–2452.

Lu, X., Yao, J., Li, C., Cui, L., Liu, Y., Liu, X., ... Li, C. (2022). Shexiang Tongxin Dropping Pills promote macrophage polarization-induced angiogenesis against coronary microvascular dysfunction via PI3K/Akt/mTORC1 pathway. *Frontiers in Pharmacology, 13*, 840521.

Mitsos, S., Katsanos, K., Koletsis, E., Kagadis, G. C., Anastasiou, N., Diamantopoulos, A., ... Dougenis, D. (2012). Therapeutic angiogenesis for myocardial ischemia revisited: Basic biological concepts and focus on latest clinical trials. *Angiogenesis, 15*(1), 1–22.

Neumann, F. J., Sousa-Uva, M., Ahlsson, A., Alfonso, F., Banning, A. P., ... Benedetto, U. ESC Scientific Document Group. (2019). 2018 ESC/EACTS guidelines on myocardial revascularization. *European Heart Journal, 40*(2), 87–165.

Pitulescu, M. E., Schmidt, I., Giaimo, B. D., Antoine, T., Berkenfeld, F., Ferrante, F., ... Adams, R. H. (2017). Dll4 and Notch signalling couples sprouting angiogenesis and artery formation. *Nature Cell Biology, 19*(8), 915–927.

Pulkkinen, H. H., Kiema, M., Lappalainen, J. P., Toropainen, A., Beter, M., Tirronen, A., ... Laakkonen, J. P. (2021). BMP6/TAZ-Hippo signaling modulates angiogenesis and endothelial cell response to VEGF. *Angiogenesis, 24*(1), 129–144.

Sabatine, M. S., Cannon, C. P., Gibson, C. M., López-Sendón, J. L., Montalescot, G., ... Theroux, P. CLARITY-TIMI 28 Investigators. (2005). Addition of clopidogrel to aspirin and fibrinolytic therapy for myocardial infarction with ST-segment elevation. *The New England Journal of Medicine, 352*(12), 1179–1189.

Sanders, L. N., Schoenhard, J. A., Saleh, M. A., Mukherjee, A., Ryzhov, S., McMaster Jr, W. G., ... Hatzopoulos, A. K. (2016). BMP antagonist Gremlin 2 limits inflammation after myocardial infarction. *Circulation Research, 119*(3), 434–449.

Sartori, R., Hagg, A., Zampieri, S., Armani, A., Winbanks, C. E., Viana, L. R., ... Sandri, M. (2021). Perturbed BMP signaling and denervation promote muscle wasting in cancer cachexia. *Science Translational Medicine, 13*(605), eaay9592.

Sasaki, H., Fukuda, S., Otani, H., Zhu, L., Yamaura, G., Engelman, R. M., ... Maulik, N. (2002). Hypoxic preconditioning triggers myocardial angiogenesis: A novel approach to enhance contractile functional reserve in rat with myocardial infarction. *Journal of Molecular and Cellular Cardiology, 34*(3), 335–348.

Sun, T., Wan, D., Song, H., & Sun, S. (2013). The effect of rosuvastatin on the expression of miR-126 and vascular regeneration in infarcted tissue after acute myocardial infarction in rats. *Journal of Zhengzhou University (Medical Edition), 48*(5), 640–643.

Todorova, D., Simoncini, S., Lacroix, R., Sabatier, F., & Dignat-George, F. (2017). Extracellular vesicles in angiogenesis. *Circulation Research, 120*(10), 1658–1673.

Wang, X., & Wu, C. (2022). Tanshinone IIA improves cardiac function via regulating miR-499-5p dependent angiogenesis in myocardial ischemic mice. *Microvascular Research, 143*, 104399.

Xia, K., Wang, Q., Li, C., Zeng, Z., Wang, Y., & Wang, W. (2017). Effect of QSKL on MAPK and RhoA pathways in a rat model of heart failure. *Evidence-Based Complementary and Alternative Medicine, 2017*, 3903898.

Yang, X., Wang, Q., Zeng, Z., Zhang, Q., Liu, F., Chang, H., ... Wang, Y. (2020). The protective effect of Qishen Granule on heart failure after myocardial infarction through regulation of calcium homeostasis. *Evidence-Based Complementary and Alternative Medicine, 2020*, 1868974.

Zeng, Z., Wang, Q., Yang, X., Ren, Y., Jiao, S., Zhu, Q., ... Wang, W. (2019). Qishen Granule attenuates cardiac fibrosis by regulating TGF-β /Smad3 and GSK-3β pathway. *Phytomedicine: International Journal of Phytotherapy and Phytopharmacology, 62*, 152949.

Zhang, H., & Bradley, A. (1996). Mice deficient for BMP2 are nonviable and have defects in amnion/chorion and cardiac development. *Development (Cambridge, England), 122*(10), 2977–2986.

Zhang, Q., Shi, J., Guo, D., Wang, Q., Yang, X., Lu, W., ... Wang, W. (2020). Qishen Granule alleviates endoplasmic reticulum stress-induced myocardial apoptosis through IRE-1-CRYAB pathway in myocardial ischemia. *Journal of Ethnopharmacology, 252*, 112573.

Zuo, W. H., Zeng, P., Chen, X., Lu, Y. J., Li, A., & Wu, J. B. (2016). Promotive effects of bone morphogenetic protein 2 on angiogenesis in hepatocarcinoma via multiple signal pathways. *Scientific Reports, 6*, 37499.